INTRAMITOCHONDRIAL FILAMENTOUS BODIES IN THE THICK LIMB OF HENLE OF THE RAT KIDNEY

TERUO SUZUKI and F. K. MOSTOFI

From the Genitourinary Pathology Branch, Armed Forces Institute of Pathology, Washington, D. C.

ABSTRACT

"Intramitochondrial filamentous bodies" (IMFB) were occasionally found within the matrix of some mitochondria of the thick limb of Henle of the rat kidney, but not elsewhere in the tubular system. Three types were recognized: type I, an accumulation of filaments 55 A thick; type II, a bundle of parallel filaments having the same thickness as those of type I and regular spacing, 87 A apart, from center to center; and type III, consisting of type II with regular light bands of 280 A periodicity and a helical border of prismatic tubular cristae. In addition to these, electron-opaque masses showing variable and faint substructures were found in the matrix of mitochondria. It is suggested that all these IMFB may originate from mitochondrial cristae and that type II IMFB may be an intermediate developmental form between type I and type III. After uranyl acetate staining, IMFB and the membranes of prismatic tubular cristae showed highly increased electron opacity. The literature has been reviewed for reports of intramitochondrial filamentous inclusions in various types of cells. These inclusions have been classified according to their structural characteristics and the localization in the mitochondria and compared with IMFB reported herein.

INTRODUCTION

The occasional occurrence of unusual intramitochondrial inclusions has been reported recently in a number of cell types from various species of organisms. Of these inclusions, the most frequent are those showing fibrillar or filamentous subunits. The only report of such findings in the kidney is by Battifora et al. (4), who observed them in magnesium-deprived rats. Unfortunately, the details of the inclusion and the segment of the tubule where they were located were not clarified. During the course of an electron microscopic study of early tubular changes of rat kidney following subcutaneous injection of glycerin,[1] we have occasionally found well-organized filamentous structures within the matrix of mitochondria in the epithelial cells of the thick limb of Henle of both experimental and control animals. In the present paper, the structural details of the "intramitochondrial filamentous bodies" (IMFB) seen in the tubular epithelia of the thick limbs of Henle will be described and compared with similar inclusions reported in many types of cells and organisms.

[1] Suzuki, T., and F. K. Mostofi. 1967. Electron microscopic studies of acute tubular necrosis. II. Early changes as seen in the thick and the thin limbs of Henle, distal convoluted tubules and collecting tubules. Manuscript in preparation.

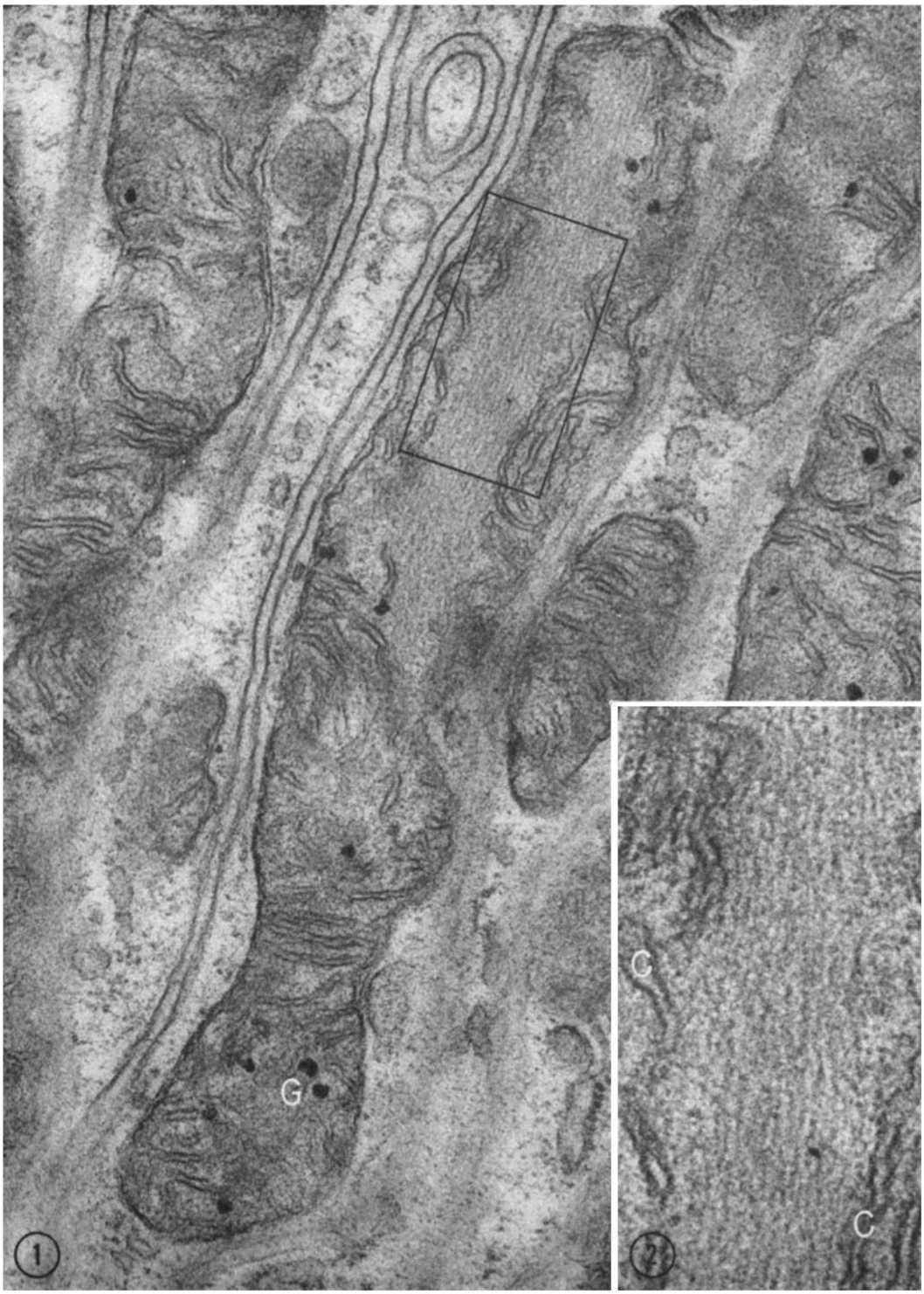

FIGURE 1 Part of epithelial cell in the thick limb of Henle from a glycerin-injected rat showing a type I intramitochondrial filamentous body (IMFB). In the upper half of this mitochondrion, located in the center of the micrograph, are a number of intramatrical filamentous structures displacing cristae. *G*, mitochondrial granules. × 54,000.

FIGURE 2 Enlargement of a part of Fig. 1 showing the detail of the filamentous structures. The average thickness of these filaments is 55 A. This section was stained only with lead acetate (Millonig). Note that the electron opacity of the filaments is much less than that of the membranes of cristae (*C*). × 127,000.

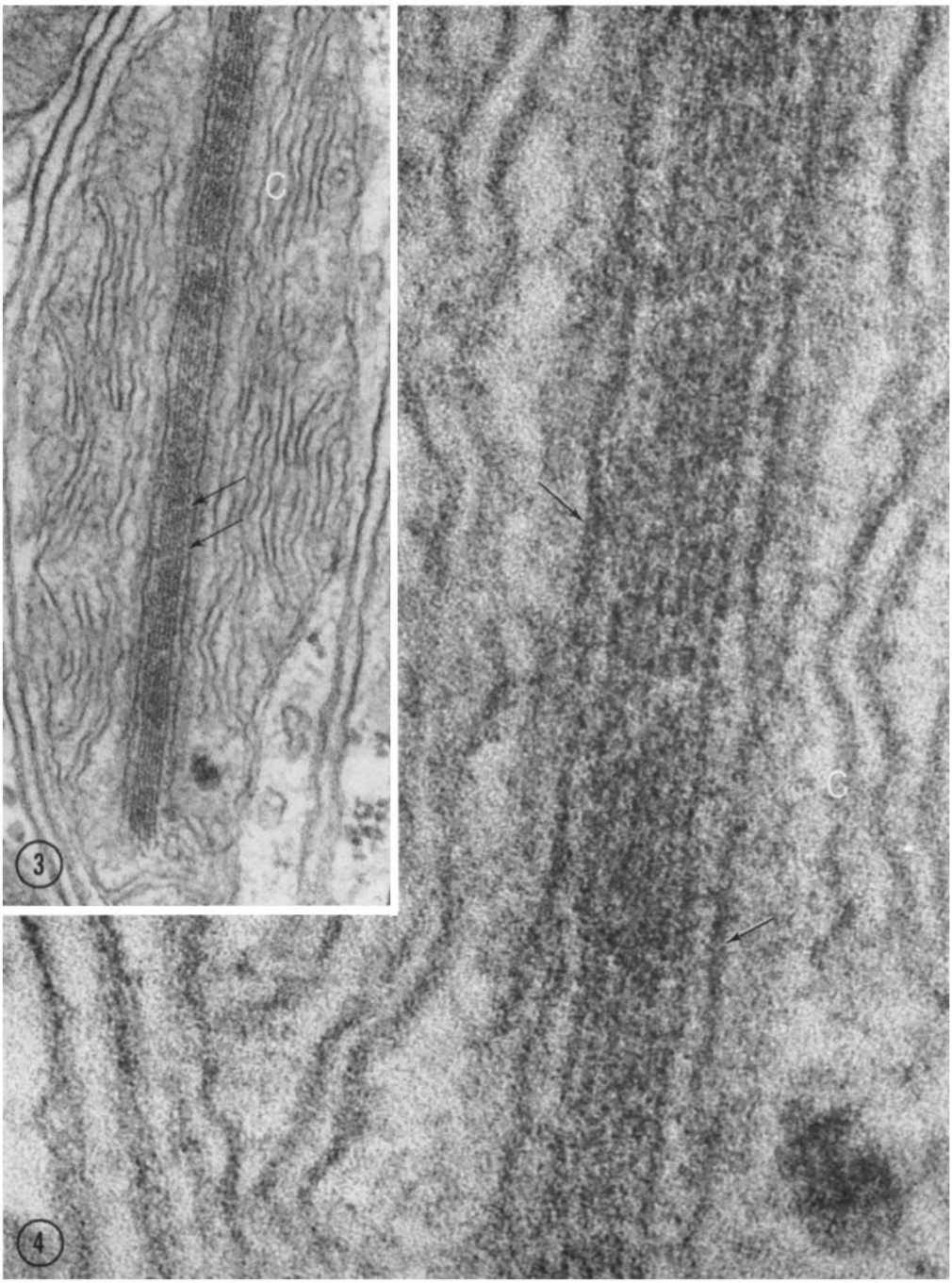

FIGURE 3 Type II IMFB in the matrix of a mitochondrion from the thick limb of Henle of a glycerin-injected rat. In this type of IMFB, the constituent filaments are parallel to each other along the long axis of the mitochondrion, forming a crystalline structure. Faint periodical bands are seen in some places (arrows). Many of the cristae (*C*) are arranged parallel to the long axes of the mitochondrion and the bundle. Double stained with uranyl acetate and lead acetate. × 80,000.

FIGURE 4 A higher power view of a part of Fig. 3. The constituent filaments are rather smooth, average 55 A in thickness, and are spaced an average distance of 87 A from center to center. The two outermost bands (arrows) of this bundle may be profiles of membranes of cristae, since they are slightly thicker, wavy, and separated by wider spaces from their neighbors than the other bands. Note that the relative electron opacity of the filaments is generally higher than that of the membranes of cristae (*C*) because of the double staining. × 331,000.

MATERIALS AND METHODS

25 rats[2] of Sprague-Dawley strain weighing 120–250 g were used.[3] 18 rats were given subcutaneously 1.75 ml/100 g body weight (B.W.) of 50% glycerin diluted with normal saline; these animals were then sacrificed at periods ranging from 15 min to 24 hr after injection. Four control animals were given the same amount of saline and sacrificed at 15 min and 2 hr after injection. No food was given for 16 hr before injection, but all animals received water ad lib. Three other animals that had had water and food ad lib. were also used for controls.

Small blocks of tissue were removed from the renal cortex and medulla after the animals were anesthetized with intraperitoneal injection of Diabutal.[4] The control animals were killed with instantaneous decapitation. The tissue blocks were immediately fixed for 2 hr in ice cold 1% osmium tetroxide adjusted at pH 7.4 with acetate-veronal buffer and at 0.34 osmol by addition of sucrose. After rapid dehydration in alcohol and propylene oxide, these specimens were embedded in either Epon (18) or Epon-Araldite mixture (47).[5] Thin sections were cut and stained with lead acetate (20), with saturated aqueous solution of uranyl acetate (45), or with both.

Electron microscopy was done with RCA-3F and Siemens Elmiskop IA microscopes.

OBSERVATIONS

Three types of intramitochondrial bodies were encountered. Type I consisted of an accumulation of dense and smooth filamentous structures with an average diameter of 55 A. They occurred in the long axis of a mitochondrion and displaced the cristae (Figs. 1, 2, 7, 17, 18).

Type II appeared as a crystal consisting of a bundle of well-organized smooth and dense filaments (Figs. 3, 4). In longitudinal sections, it consisted of many filaments of an average thickness of 55 A running parallel to each other along the long axis of a mitochondrion and spaced a distance of 87 A from center to center. Faint, periodical bands could be seen in some of them (Fig. 3).

Type III also showed a crystalline structure consisting of a bundle of regularly grouped filaments similar to those of type II in size and spacing but differing from them in two respects: (*a*) Many light bands with an average periodicity of 280 A could be seen clearly across the bundle in longitudinal sections (Figs. 5, 6, 8–10, 16). Many of these bands showed an angle of up to 28° to the short axis of the bundle (Figs. 6, 18). This, however, may be an artifact caused by distortion of the section. (*b*) In longitudinal sections, many triangular vesicular structures were arranged along the lateral sides of the grouped filaments (Fig. 6). Since many micrographs suggested a continuation between the vesicles and paired linear structures

[2] These animals were obtained from an inbred stock at the National Institutes of Health, Bethesda, Md.

[3] The "Principles of Laboratory Animal Care" as promulgated by the National Society for Medical Research were observed during this study.

[4] Diabutal, 3 mg/100 g B.W. (pentobarbital sodium, Diamond Laboratories, Inc., Des Moines, Iowa), was used.

[5] This resin was prepared in the following proportions and used for embedding instead of the ready-prepared routine epoxy mixture (18). Epon 812: 20 ml; Araldite (component A/M of Durcupan ACM, Fluka AG, Basel, Switzerland): 16 ml; DDSA: 48 ml; and DMP-30: 2.0 ml.

FIGURE 5 A low-power view of a part of the thick limb of Henle from a glycerin-injected rat. A mitochondrion bearing type III IMFB is seen in the center. *L*, tubular lumen; *Bm*, basement membrane. Section stained with lead acetate alone. × 6,400.

FIGURE 6 Higher power view of the same mitochondria and two type III IMFB shown in Fig. 5. Both of these type III bodies are present within the matrix of this mitochondrion and appear as bundles of parallel filaments comparable to those of the type II body in Figs. 3 and 4. These bundles also show light bands (arrows *a*) averaging 50 A in width and having a regular periodicity of 280 A. In this micrograph, they appear to have an angle of 5–10° to the short axis of the bodies. Triangular vesicular structures, presumably cross-section profiles of tubular and prismatic cristae (arrows *b* and *c*), are arranged on each side of a bundle. Many of the other cristae (*C*) are arranged roughly parallel to the long axes of this mitochondrion and these bodies. Because of the staining with lead acetate alone, the electron opacity of the constituent filaments is less than that of the membranes of cristae. Mitochondrial granules (*G*) appear normal. × 57,000.

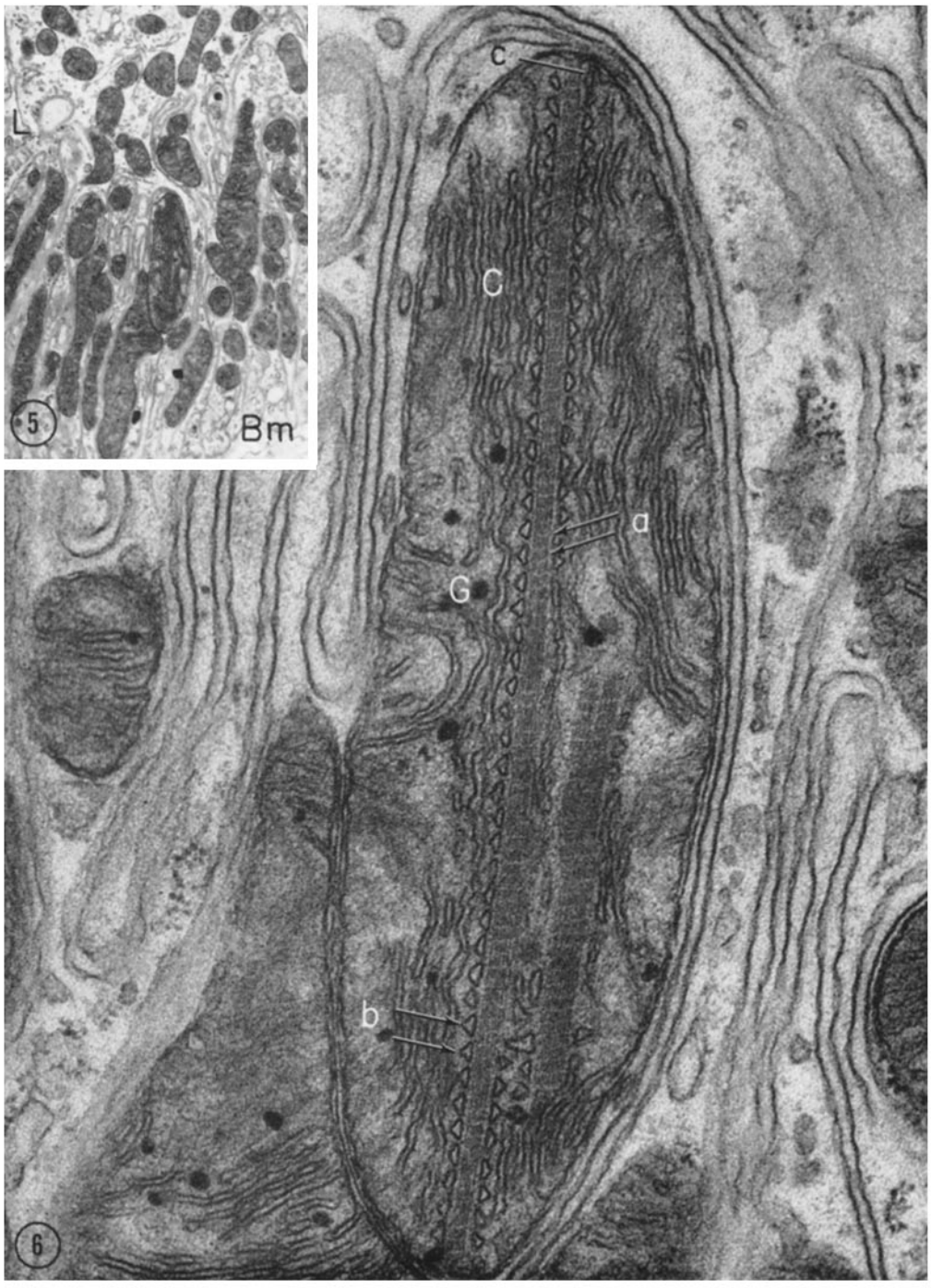
L
5
Bm
c
C
a
G
b
6

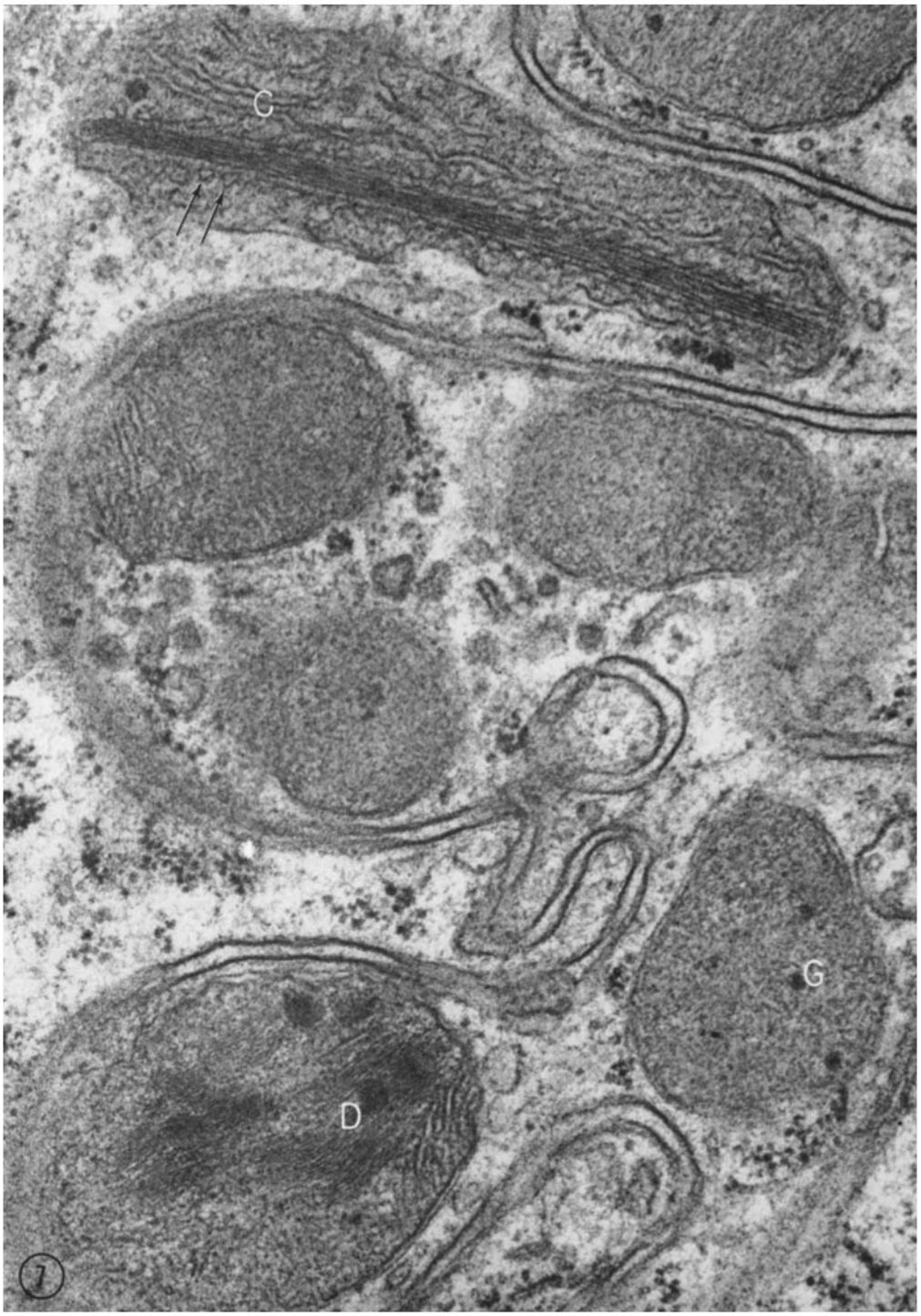

FIGURE 7 Parts of epithelial cells in the thick limb of Henle from a control rat showing two mitochondria bearing type II (upper) and type I (lower left) IMFB, respectively. In the former, no distinct periodical bands are seen, but triangular profiles of prismatic tubular cristae (arrows) are found along the bundles of filaments. The other cristae (*C*) are arranged parallel to the body and the long axis of the mitochondrion. In the lower left mitochondrion, two electron-opaque masses (*D*), which are probably different entities from regular mitochondrial granules (*G*), are recognized in association with bunched filaments. Double-stained section. × 61,000.

obliquely overlapping the bundle (Figs. 15, 16), it was assumed that these vesicles were cross-sectional profiles of prismatic cristae helically surrounding a bundle of filaments. This assumption is also supported by the results of electron staining, which will be described later. In some micrographs of type I (Fig. 17) and type III (Fig. 16) IMFB, close topographic relationships between IMFB and mitochondrial cristae suggested a possible relationship between these two structures.

The intramitochondrial filamentous bodies (IMFB) were found in all the experimental and control animals. Though it is impossible to determine the exact frequency of such bodies without studying serial sections, it was apparent in our study that these bodies were not present in every cell in a positive case nor in every mitochondrion in a positive cell.

The most frequent site was in the epithelial cells of the thick limb of Henle, where at least one profile of IMFB was detected in mitochondria included in 10–15 cross-sections of random tubules. Sometimes up to three profiles of IMFB-bearing mitochondria could be seen within a single section of the same cell. Similar bodies were rarely seen in the mitochondria of the distal convoluted tubules, thin limbs of Henle (Fig. 13), or the collecting tubules (Fig. 14) of the kidneys of glycerin-injected animals. Except for an occasional lamellar arrangement of cristae that may simulate IMFB, none have been found in the mitochondria of the proximal convoluted tubules.

There were fewer IMFB-bearing mitochondria in renal epithelial cells of control rats than in those of experimental animals. In the latter, IMFB were found both in swollen mitochondria (Fig. 12) of pathologic cells and in normal mitochondria (Fig. 6) of normal cells. Although usually occurring singly, sometimes as many as three IMFB could be seen in the same mitochondrion (Figs. 6, 8–12, 16–19).

All of the IMFB found in the present study were located within the matrix of mitochondria but not in the intracristal space or in the space between the outer and inner mitochondrial membranes.

In addition to the three types of IMFB, electron-opaque round masses measuring up to 150 mμ in diameter were located in the matrix of the mitochondria and readily distinguished from the regular mitochondrial granules (Figs. 7, 9, 10). These usually occurred in relationship to type III IMFB and less frequently in relationship to types I and II. In some of them, faint and uncertain substructures could be recognized.

In some mitochondria, two bodies showing incomplete hexagonal shapes could be found (Fig. 11). These consisted of fine granules about 55 A in diameter, spaced an average distance of 87 A from center to center. They showed an arrangement like a crystalline lattice and, since the diameter of the unit dots and their spacing corresponded well to those of the filaments, they were assumed to be cross-sectional profiles of either type II or III. In other fields, profiles of filamentous bodies with angular shapes suggesting square or parallelogrammatic columns were also found (Fig. 12).

The length of type II and III bodies was 2–4 μ, depending upon the size of the mitochondria bearing them. The mitochondria bearing IMFB were similar in their size, shape, and mitochondrial granules to those without IMFB. The cristae of the IMFB-bearing mitochondria were often but not always decreased in number. Many of the cristae were arranged parallel to the long axis of the mitochondria and the IMFB (Figs. 3, 6, 7).

After the IMFB were stained with lead acetate alone, their relative density was less than that of the transversely sectioned outer and inner mitochondrial membranes (Figs. 17, 19). After staining with uranyl acetate or double staining with uranyl acetate and lead acetate, however, the relative density of the IMFB was much greater than that of the outer and inner membranes (Figs. 18, 20). Moreover, in type III IMFB stained either doubly with uranyl acetate and lead acetate or singly with uranyl acetate, the triangular vesicles along the lateral sides (Figs. 10, 15, 20) and the pairs of linear structures obliquely overlapping the body (Fig. 15) showed considerably increased electron opacity, similar to that of the constituent filaments of the bundle.

These findings suggest that the triangular vesicles and the pairs of linear structures are different profiles of the same structure, presumably mitochondrial cristae that helically surround a bundle of the filaments but have been cut in transverse and longitudinal directions, respectively.

DISCUSSION

Intramitochondrial filamentous bodies (IMFB) and other similar structures of varying sizes and shapes have been found, by various investigators, in the matrix, within dilated intracristal spaces, or

in the space between the outer and inner membranes of the mitochondria of many types of cells and species of organisms (Table I). Well-organized parallelism with even spacing, regular periodical bands, and images suggesting a helical architecture have been noted in filamentous structures described in these reports. On the basis of the description in various reports, these intramitochondrial filamentous inclusions can be divided (Table I) into two main categories: those occurring in the matrix (references 1, 2, 4, 6–8, 13, 16, 17, 22, 23, 25–27, 31, 32, 34, 36, 39, 42, 44, 46, and this report); and those occurring in the intracristal space and the space between the outer and inner mitochondrial membranes (references 3, 15, 23, 24, 33, 37, 43 and footnote 6). Each group can be further classified into: neither periodical nor helical, *A-1* (references 1, 2, 6–8, 13, 16, 17, 22, 23, 25–27, 31, 32, 34, 36, 39, 42, 44, 46, and this report), and *B-1* (reference 3); periodical, *A-2* (this report), and *B-2*,[6] and helical, *A-3* (reference 4), and *B-3* (references 15, 23, 24, 33, 37, 43). Subgroup *A-1* can be divided still further into two subgroups: *A-1-a*, those consisting of single or accumulated filaments (references 1, 2, 8, 17, 23, 26, 27, 31, 32, 39, and this report), and *A-1-b*, those consisting of parallel filaments (references 6, 7, 13, 16, 22, 25, 34, 36, 42, 44, 46, and this report). According to this classification, IMFB types I, II, and III belong to *A-1-a*, *A-1-b*, and *A-2* groups, respectively, with type II constituting an intermediate form between types I and III.

It should be mentioned that to date, except for a doubtful case reported by Battifora et al. (4), all inclusions showing a clear helical architecture have been found within the intracristal space (Table I, *B-3* group), but not within the matrix. In contrast, all the IMFB types I, II, and III reported in this study were located in the matrix. It should be mentioned that filamentous inclusions comparable to each type of IMFB have been observed individually.

Since our type II IMFB showed certain morphologic features common to both type I and type III, is it possible that many of the filamentous inclusions of groups *A-1-a*, *A-1-b*, and *A-2* that have been reported independently may be related to each other or even represent different stages in the development of the same structure?

A few reports are available in the literature that mention intramitochondrial inclusions that closely resemble our types II and III IMFB. Battifora et al. (4) reported intramitochondrial inclusions similar to type III in the tubular epithelial cells of magnesium-deprived rats that they designated as "intramitochondrial helical bodies," but they did not define the specific location in the tubules.

The "type 2 inclusion body" of Ebe et al. (6) consisted of parallel filaments 75 A thick and 70–80 A apart. It was found in the matrix of mitochondria in urinary epithelium of the striped snake (*Elaphe quadrivirgata*). It was similar to type II of the present study, but the constituent filaments of the latter were more smooth than those of the former and did not show a granular appearance in detail (Fig. 4).

"Crystalline inclusions" found by Svoboda and Manning (42) in hepatic cell mitochondria from a patient with chronic alcoholism and "filamentous inclusions" observed by Mugnaini (22) in hepatic cell mitochondria from a normal 20-yr-old man and from a patient with alcoholic dyspepsia also resemble type II and III bodies of the present study. The parallel filaments of the "crystalline inclusion" of Svoboda and Manning, however, were 120 A thick and 200 A apart. Their mitochondria also contained "large matrix granules" resembling our dense intramatrical masses. On the other hand, the filaments of the "filamentous inclusion" of Mugnaini were 60 A thick and 60 A apart.

[6] Price, H. M., G. B. Gordon, T. L. Munsat, and C. M. Pearson. 1967. Myopathy with atypical mitochondria in the (Type I) skeletal muscle fibers. *J. Neuropathol. Exptl. Neurol.* In press.

FIGURE 8 High-power view of two type III IMFB in the matrix of a mitochondrion of the thick limb of Henle from a rat with subcutaneous injection of glycerin. They show periodical light bands (arrows) characteristic of this type of body. The average dimensions of these bodies are as follows: thickness of the constituent filament: 55 A; space between the filaments (center to center): 87 A; width of the light bands: 50 A; width of the dark bands: 230 A; and periodicity of the bands: 280 A. The section was doubly stained. × 122,000.

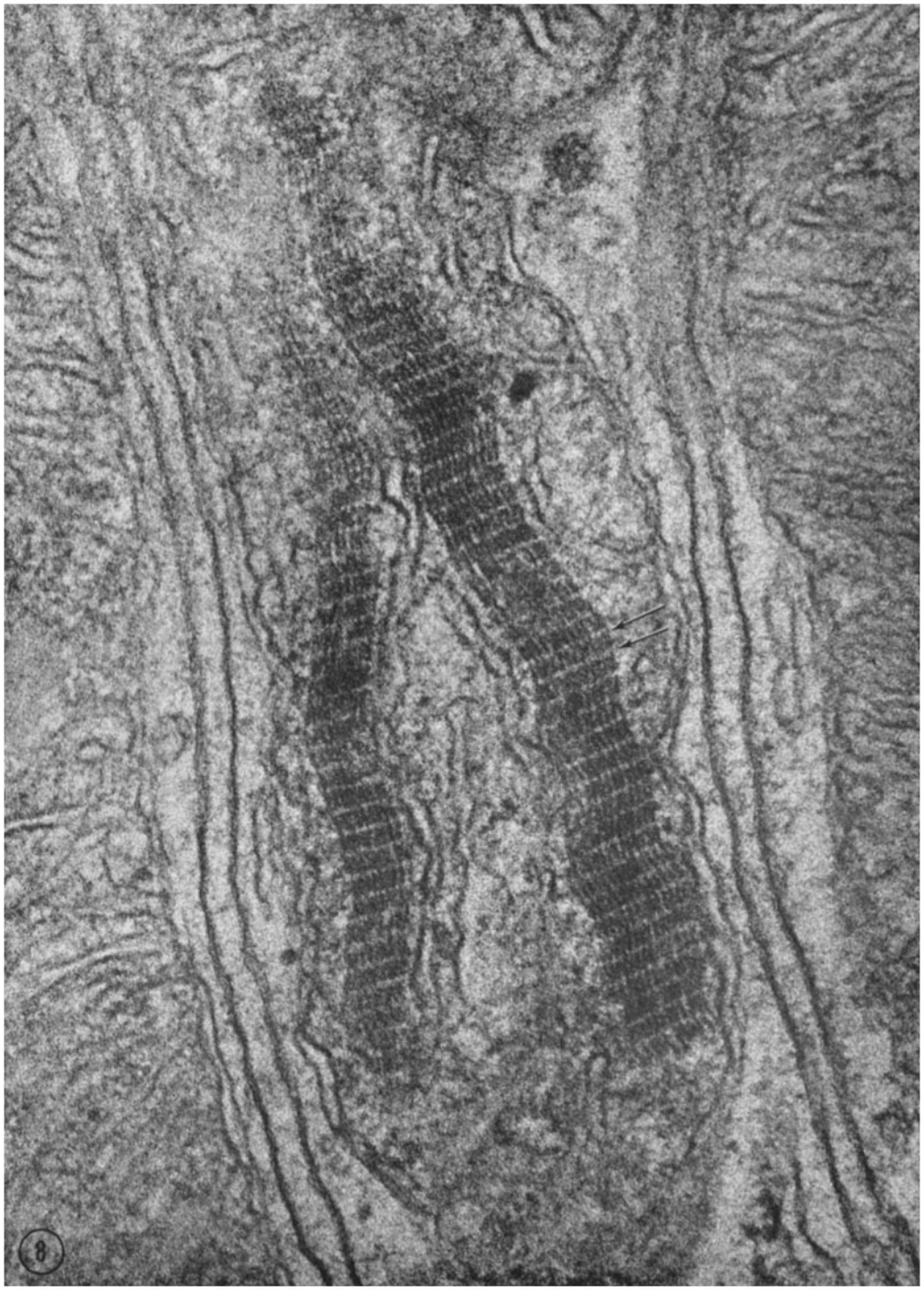

TABLE I

Classification of Intramitochondrial Filamentous Inclusions

Location	Morphological Character		Type of cell	Species	References
A. Matrix	1. Neither periodical nor helical	a. Single or accumulated filaments	Oocyte	Guinea pig	1
			Oocyte	Guinea pig	2
			Protozoa	*Tetrahymena pyriformis*	8
			Hepatic cell	Human, idiopathic diabetes mellitus	17
			Astrocyte	Rat	23
			Embryonic cell	Chick	26
			Embryonic cell	Chick	27
			Ameba	*Amoeba pelomyxa*	31
			Ameba	*Amoeba pelomyxa*	32
			Glial cell	Amphibia	39
			Kidney tubule	Rat	This report
		b. Parallel filaments	Kidney tubule	Striped snake	6
			Hepatic cell	Human cholestasis	7
			Thyroid, follicular cell	Rat, with stimulator and inhibitor	13
			Hepatic cell	Human, viral hepatitis*	16
			Hepatic cell	Human, normal and with alcoholic dyspepsia	22
			Brown adipose tissue	Mouse and rat	25
			Hepatic cell	Human, chlorpropamide administration	34
			Hepatic cell	Human, acute alcoholic hepatitis	36
			Hepatic cell	Human, chronic alcoholism	42
			Hepatic cell	Human and mouse, amyloidosis	44
			Hepatic cell	Human, normal	46
			Kidney tubule	Rat	This report
	2. Periodical		Kidney tubule	Rat	This report
	3. Helical		Kidney tubule	Rat, magnesium deprivation‡	4
B. Intracristal space and space between outer and inner mitochondrial membranes	1. Neither periodical nor helical		Spermatocyte	*Testacella*	3
	2. Periodical		Skeletal muscle cell	Human, pathologic	§
	3. Helical		Hepatic cell	Rat, prolonged ethanol ingestion	15
			Astrocyte	Rat	24
			Astrocyte	Rat	23
			Slime mold	*Didymium nigripes*	37
			Hepatic cell	Rat, protein deficiency	43
			Hepatic cell	Rat, chronic alcoholism	33

* Iezequel assumed this inclusion to be a lamellar structure. ‡ This inclusion probably belongs to group *A-2*.

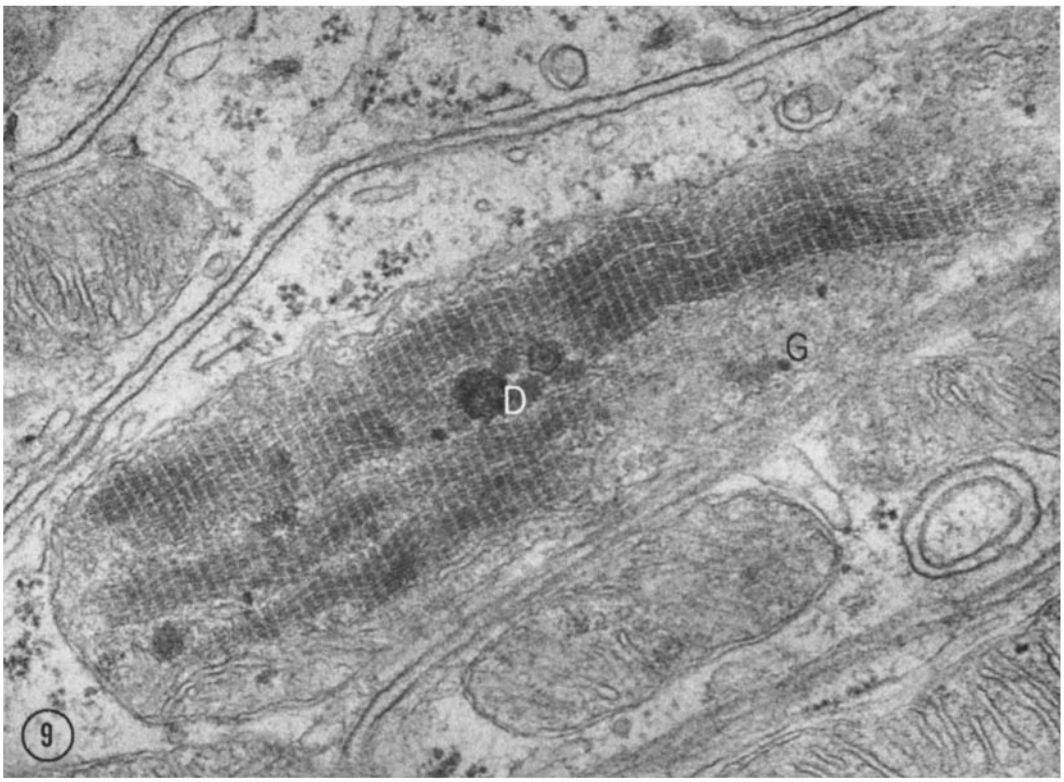

FIGURE 9 A mitochondrion from the thick limb of Henle in a glycerin-injected rat. Several type III IMFB and dense intramatrical masses (*D*) different from regular mitochondrial granules (*G*) are seen in this mitochondrion. Double-stained section. × 56,000.

In both reports, many transversely sectioned vesicular profiles, presumably of mitochondrial cristae, were arranged adjacent to the bundle of the filaments. Neither report, however, showed regular periodical bands like those seen in the "helical body" of Battifora et al. (4) and in the type III body of the present study, and no one has demonstrated images suggestive of a helical border of tubular and prismatic cristae around the filaments of bundles. Accordingly, it seems to us that, among all the group *A* intramitochondrial filamentous inclusions, type III IMFB appear to have the most intricate architecture.

In a study of liver cells from a patient with epithelioma of the bile duct and prolonged viral hepatitis, Jezequel (16) reported intramitochondrial bodies and suggested that these inclusions consisted of myelin-like lamellae and were derived from the membranes of mitochondrial cristae. We believe, however, that her inclusions closely resemble those reported by Svoboda and Manning (42) and Mugnaini (22) and probably consist of filaments and not lamellae. Svoboda and Manning (42) believed that their "crystalline inclusion" was derived from the membranes of cristae and was related to disordered phospholipid metabolism in mitochondria.

Fujita and Machino (13) found "intramitochondrial crystals" comparable to our type II in follicular cells of the rat thyroid following administration of thyroid stimulators and inhibitors. Since there were fewer cristae in such mitochondria, especially in the area around the "crystal," they assumed that the "crystals" originated from mitochondrial cristae.

Since cristae contain considerable amounts of phospholipid and since myelin-like structures are actually derived from phospholipid in in vitro experiments (9–11, 40), it is quite logical to assume that the inclusions originate from the membrane of cristae. In the present study, close topographic relationships between IMFB and mitochondrial

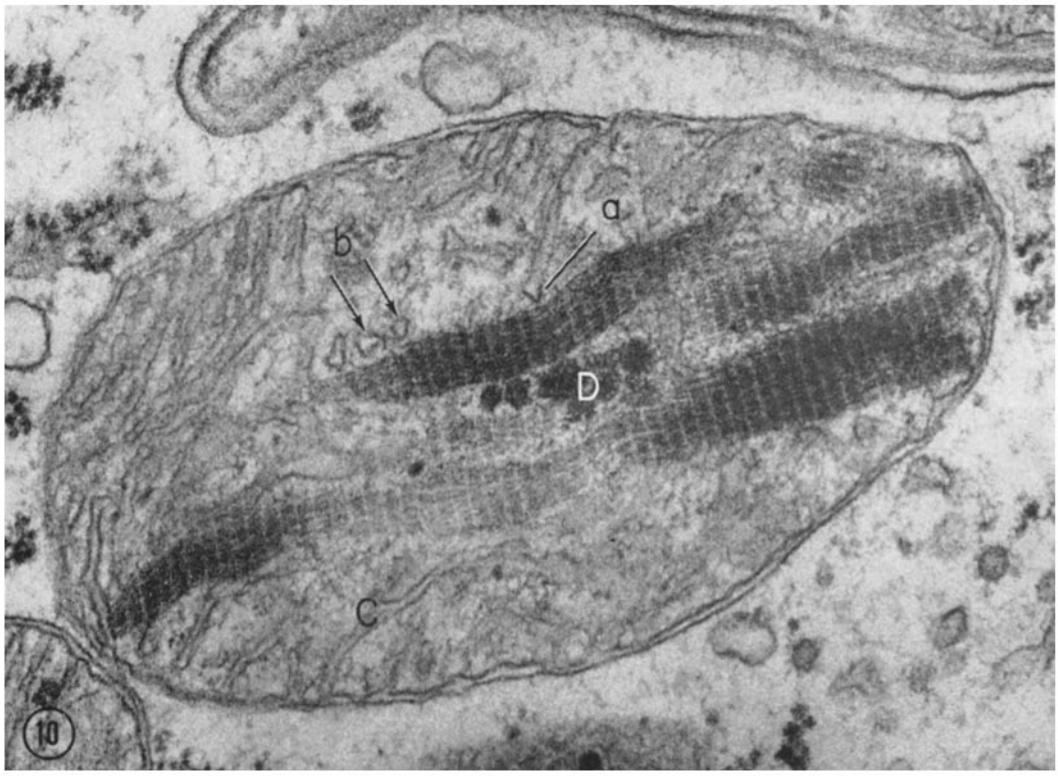

FIGURE 10 A mitochondrion from the thick limb of Henle in a glycerin-injected rat showing type III IMFB and unidentified dense intramatrical masses (*D*). The relative electron opacity of these bodies is generally higher than that of the membranes of cristae (*C*). Note that V-shaped tip of a crista (arrow *a*) located close to the body shows a very much increased electron opacity, which is also seen in some other triangular profiles of cristae (arrows *b*). Double-stained section. × 77,000.

cristae were also found in some fields, suggesting a possible origin of IMFB from mitochondrial cristae. A helical border of prismatic cristae that showed increased electron opacity after uranyl acetate staining, however, would also indicate a close relationship between IMFB and the altered cristae. The significance of such an arrangement of cristae is not known.

Mitochondria showing prismatic cristae have been demonstrated in various cells of many animal species by Revel et al. (35), in astrocytes of the cat by Mugnaini and Walberg (23), and in astrocytes of the hamster by Blinzinger et al. (5). Such a peculiar transformation and uniform rearrangement of prismatic and helical cristae may suggest a specialized metabolic activity different from the usual functions of the mitochondria.

In a study of experimental amyloidosis of mice, Sorenson et al. (38) demonstrated an accumulation of amyloid filaments 100 A thick within the mitochondrial matrix of the Kupffer cell of the liver. The general appearance of the mitochondria with amyloid filaments is quite similar to that of mitochondria with our type I body, but the thickness of the constituent filaments in the type I body is nearly half that of the amyloid filaments, and the two can be easily differentiated.

Considering the chemical nature of IMFB, it should be noted that after these bodies were stained with uranyl acetate they showed considerably increased electron opacity in comparison to the membranes of mitochondria. As reported by Huxley and Zubay (14) and Stoeckenius (41), this may denote the possible presence of nucleic acid in the IMFB.

Two other reports merit consideration. In the

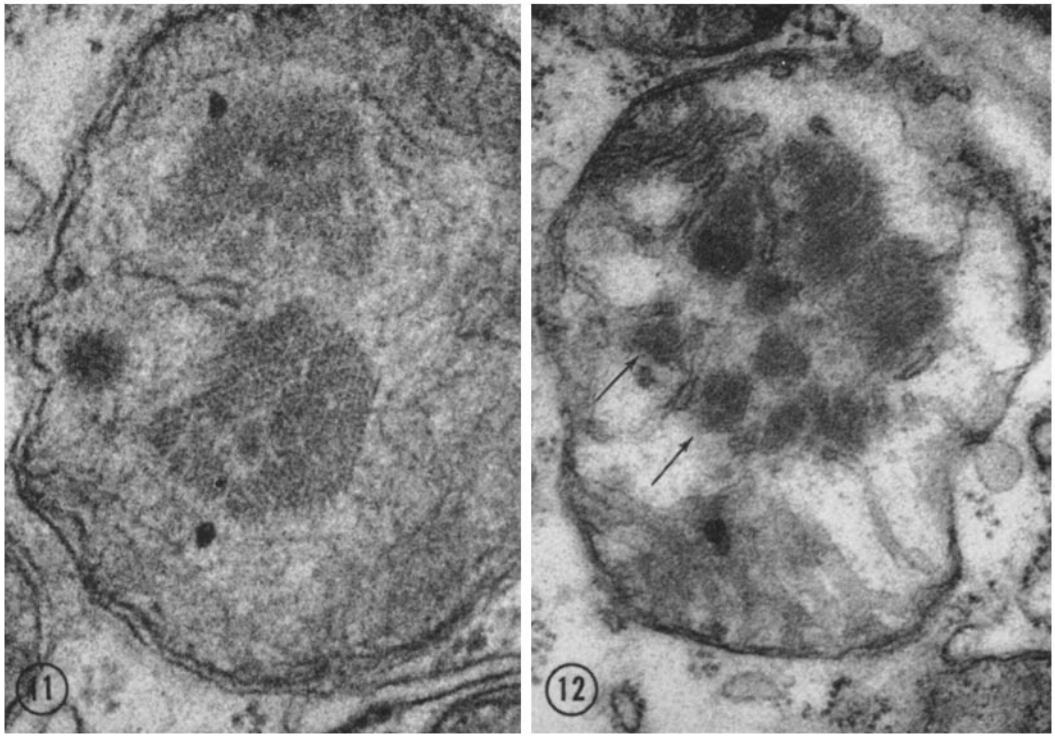

FIGURE 11 A transversely cut type II or III IMFB suggesting a hexagonal shape, in a mitochondrion from the thick limb of Henle of a glycerin-injected rat. In this plane, the constituent filaments appear as a number of dots arranged regularly with a certain spacing comparable to the dimension in IMFB filaments shown in Figs. 4, 6, and 8. × 89,000.

FIGURE 12 In another glycerin-injected rat, angular shapes of IMFB are also noted from their transversely or obliquely sectioned profiles (arrows). These two micrographs suggest that IMFB consist of filamentous structures and not lamellae. The sections were stained with lead acetate alone. × 57,000.

study of mitochondria from embryonic cells of the chick, Nass and Nass (27, 28) reported that intramatrical filamentous inclusions in such cells showed increased electron opacity after staining with uranyl acetate. These inclusions were removed by DNase digestion but not by RNase and pepsin treatment, leading to the conclusion that the filamentous inclusions in the mitochondrial matrix of the chick embryo were rich in DNA. Similar results have been reported by Schuster (37) on the "coiling intracristal fibrillar core" of the slime mold (*Didymium nigripes*). The location of intramitochondrial inclusions is an important factor in determining their nature, since it indicates the specific enzymatic environments and the different metabolic conditions. These reports indicate, however, that DNA-containing filaments can appear in the matrix of the mitochondria as well as in the intracristal spaces and that differences in location do not necessarily mean differences in chemical composition.

The more frequent appearance and larger size of the "intramitochondrial inclusion bodies" in the urinary epithelium of the striped snakes that were in their active season led Ebe et al. (6) to claim that these bodies indicated an altered metabolic activity of the mitochondria. Wills (46) thought that "crystalline structures" found in normal human hepatic cells were a variant of normal hepatocyte mitochondria and that their presence in some cells was a reflection of a functional heterogeneity among the cells within each lobule of the liver, as has been established for the distribution of certain enzymes. Mugnaini (24)

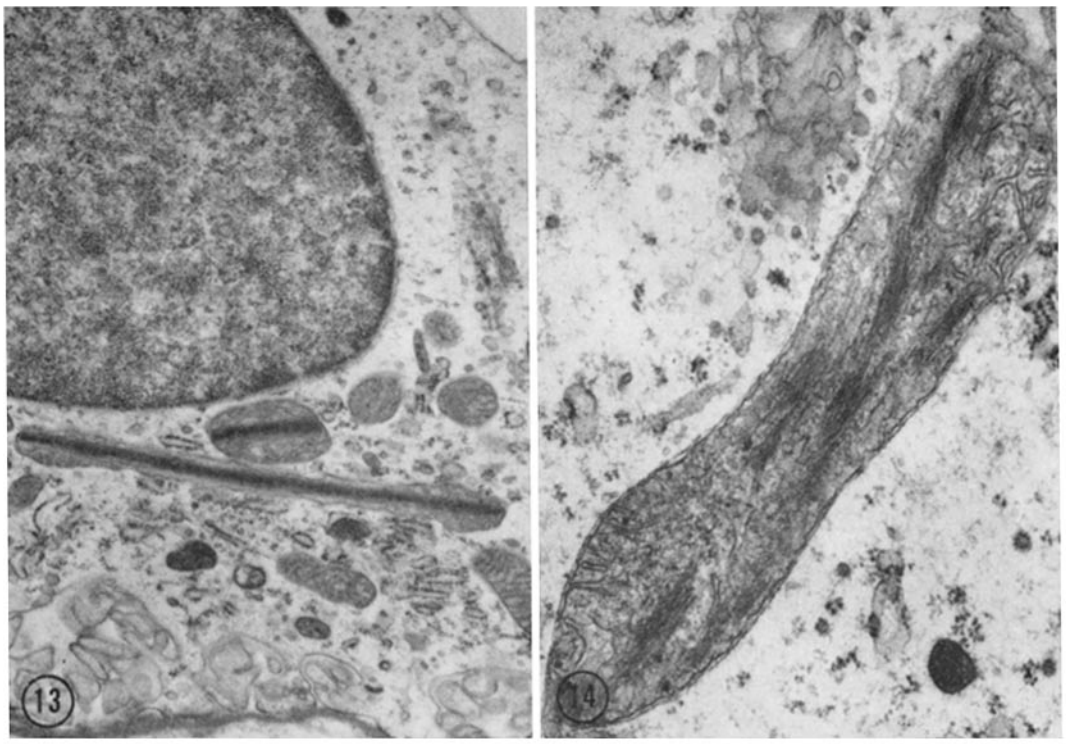

FIGURE 13 Part of an epithelial cell of the thin limb of Henle from a glycerin-injected rat. Two mitochondria show inclusion bodies similar to type II or III IMFB as seen in the thick limb of Henle. Double-stained section. × 16,000.

FIGURE 14 A mitochondrion from an epithelial cell of the collecting tubules of a glycerin-injected rat, showing intramatrical filamentous structures similar to type I IMFB as seen in the thick limb of Henle. Double-stained section. × 37,000.

described "helical filaments" in the intracristal spaces of astrocytic mitochondria from a normal rat; he believed that these represented a particular phase of mitochondria. In another paper (22) on "filamentous inclusions" in the matrix of human hepatic cell mitochondria, however, he considered them to represent a nonspecific reaction of the mitochondria to cell injury, probably as a consequence of interference with some basic enzymatic activity. Svoboda and Manning (42), too, suggested that the appearance of the "crystalline inclusions" in mitochondria of pathologic human hepatic cells represented a nonspecific degenerative phenomenon.

FIGURE 15 A part of an epithelial cell in the thick limb of Henle from a glycerin-injected rat. Two mitochondria show obliquely (upper right) and longitudinally (left half) sectioned IMFB. In the latter, a type III body, cross-sectioned profiles of prismatic cristae (arrows *a*) arranged longitudinally on both sides of the bundle are seen in the upper third of this body. In the lower third, pairs of parallel lines (arrows *b*) transverse the bundle. In some parts (arrows *c*, *d*, and *e*), continuation between the membranes of tubular and prismatic cristae and paired cross lines is suggested. These findings, also shown in Figs. 6, 10, and 16, suggest that tubular cristae of prismatic shape surround the bundle of filaments helically. Double-stained section. *G*, mitochondrial granule; *N*, nucleus. × 68,000.

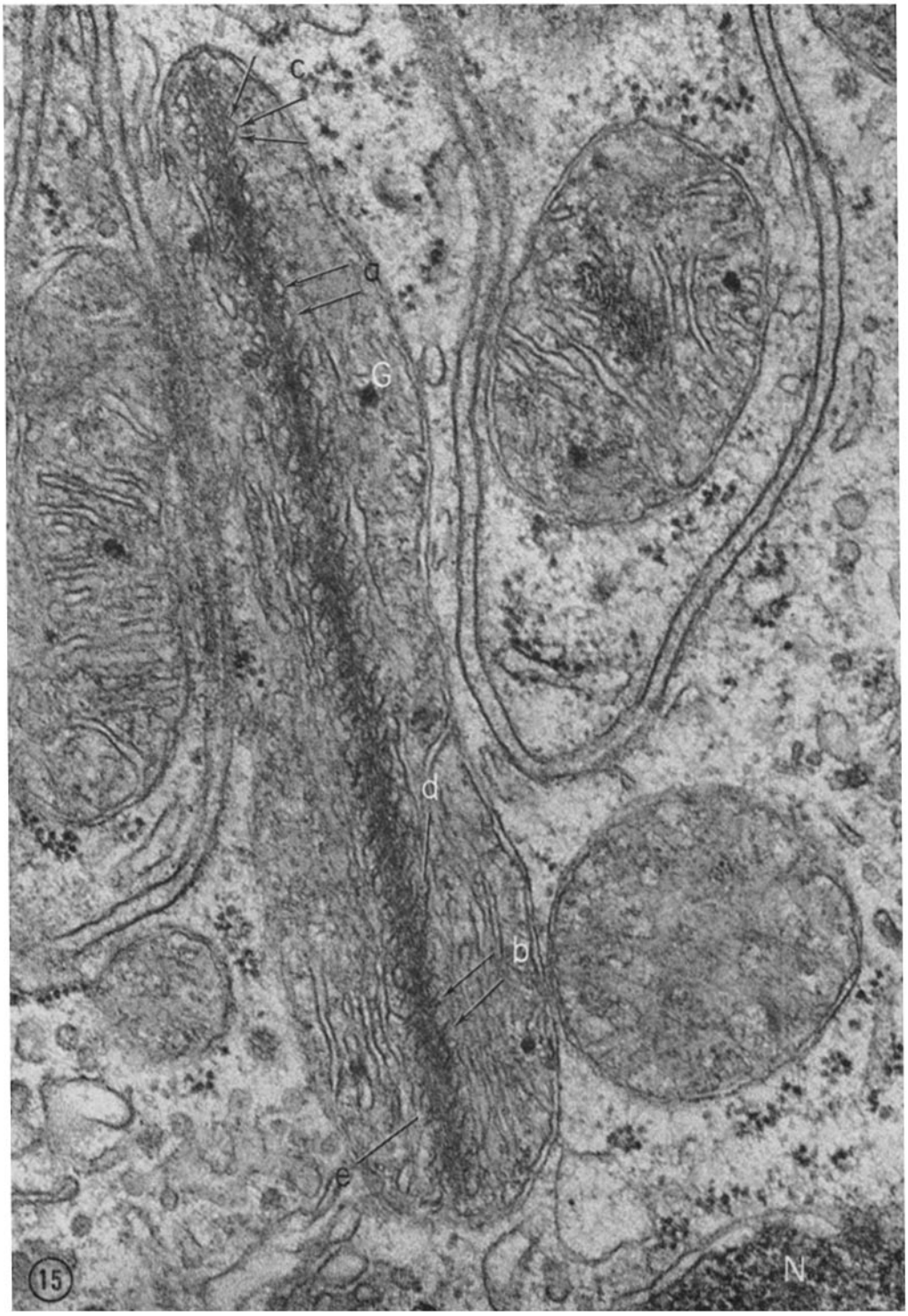
c
a
G
d
b
e
N
15

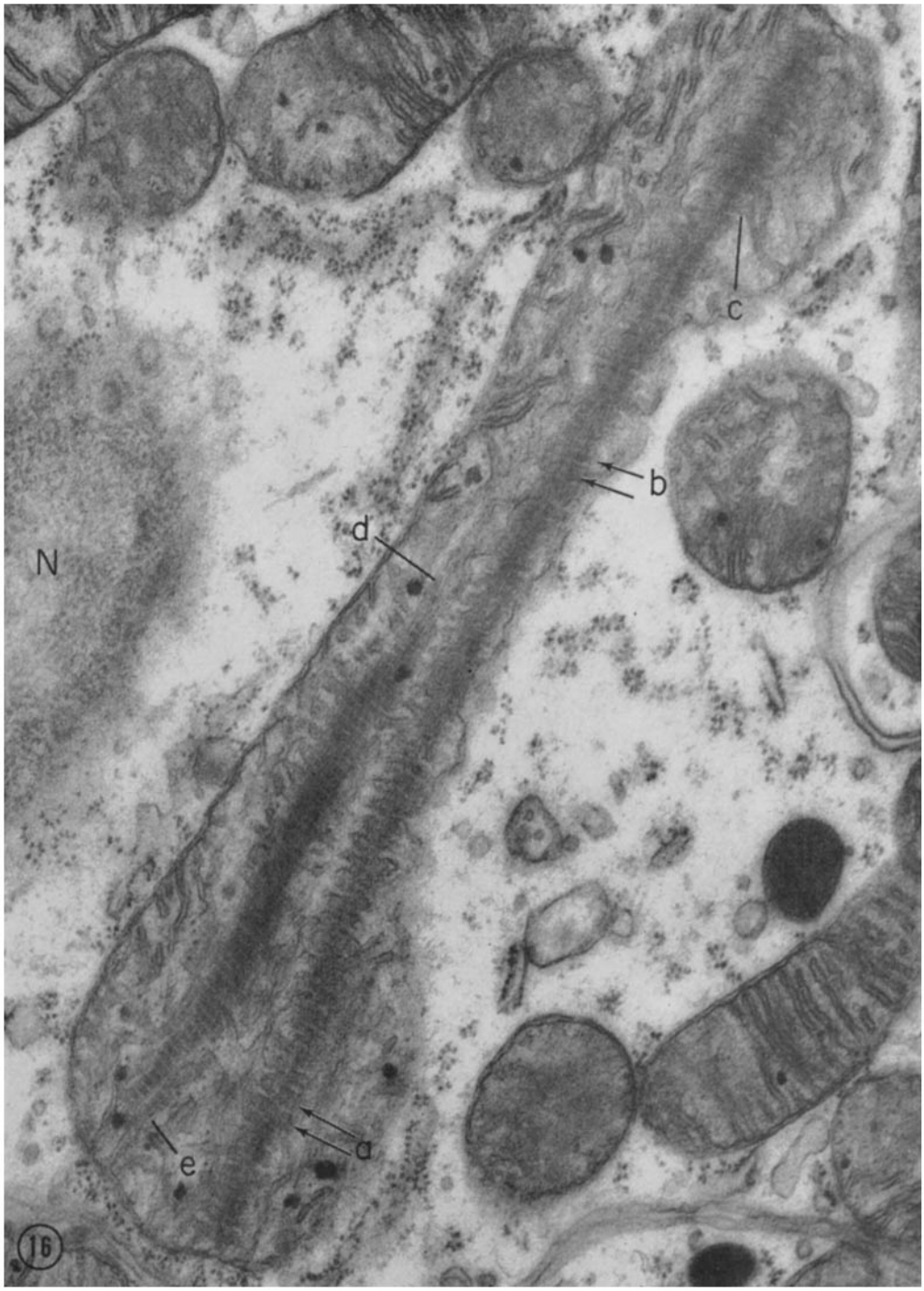

FIGURE 16 A mitochondrion in an epithelial cell of the thick limb of Henle from a glycerin-injected rat. This mitochondrion bears two type III IMFB. In the one on the right, note the arrangement of tubular membranes (arrows *a* and *b*) across the bundle of the constituent filaments. Many of these tubular membranes show a width greater than that of regular cristae, and one of these (arrow *c*) appears continuous with a crista that is seen as an infolding of the inner membrane of this mitochondrion. Also note close topographic relationship between IMFB and cristae at two points (arrows *d* and *e*), suggesting a possible origin of IMFB filaments from the cristae. *N*, nucleus. Section stained with lead acetate alone. × 48,000.

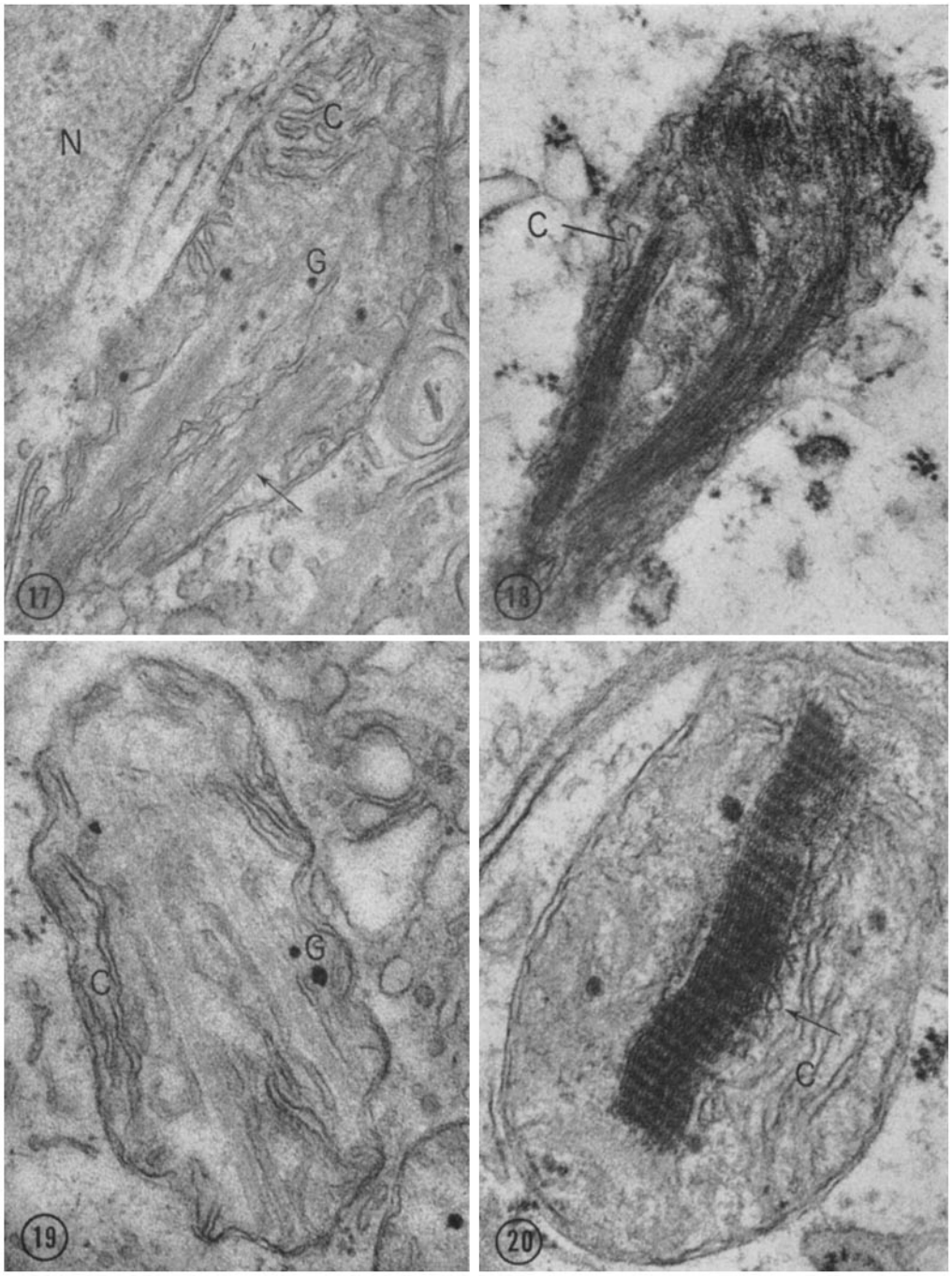

FIGURES 17, 18, 19, and 20 All of these micrographs are of the thick limbs of Henle of four glycerin-injected rats. The sections in Figs. 17 and 19 were stained lightly with lead acetate alone, while those in Figs. 18 and 20 were doubly stained with uranyl acetate and lead acetate. Note that the relative electron-opacities of the type I and II IMFB in Figs. 17 and 19 are much less than those of the membranes of mitochondrial cristae (*C*). On the other hand, the relative densities of the type I and III IMFB in Figs. 18 and 20 are much higher than those of the membranes of the cristae, suggesting a possible presence of nucleic acid in the IMFB. Also note in Fig. 20 that triangular cristae (arrow) arranged on the surface of the type III IMFB show much increased electron-opacity, comparable to that of the constituent filaments. In Fig. 17, a crista of this mitochondrion shows loss of membrane at the tip (arrow), where it merges in bunched filaments of type I IMFB, suggesting a possible origin of the filaments from cristae. *G*, mitochondrial granules; *N*, nucleus. Fig. 17, × 35,000; Fig. 18, × 59,000; Fig. 19, × 44,000; Fig. 20, × 74,000.

Other reports (16, 17, 33, 36, 43) are also available relating the appearance of intramitochondrial inclusions to a pathologic condition of the mitochondria or the cells. We have observed the inclusions not only in pathologic conditions but in control animals as well. It must be admitted, however, that the appearance of IMFB does not necessarily indicate some pathologic phenomenon, since there must be a constant turnover and natural cell death in normal organisms.

The round masses of high electron-opacity that were present in the mitochondrial matrix may be comparable to the "type 1 inclusion body" of Ebe et al. (6), "large granules" of Svoboda and Manning (42), "intramitochondrial mass" of Elliott and Bak (8), and other structures of similar names reported by many authors (12, 19, 21, 29, 30). Since these inclusions are quite different structurally from our IMFB, they are not considered in this discussion. There is need, however, for the study of these inclusions to clarify their nature and relationship to IMFB, regular mitochondrial granules, and other miscellaneous depositions in mitochondria.

A number of questions remain unanswered. What are the specific nature and function of IMFB? Why are the IMFB located mostly in the mitochondria of the thick limb of Henle? Are they specific entities in the rat, and is there any relationship between their limited localization and the special function in the physiology of this segment? The answers to these questions are not as yet known, and further studies will be needed.

This investigation was supported in part by a research contract, Project No. USARD-DA 49-193-ND 2379, from the Medical Research and Development Command, United States Army, Washington, D. C.

Received for publication 1 November 1966.

REFERENCES

1. ADAMS, E. C., and A. T. HERTIG. 1964. Studies on guinea pig oocytes. I. Electron microscopic observations on the development of cytoplasmic organelles in oocytes of primordial and primary follicles. *J. Cell Biol.* **21**:397.
2. ANDERSON, E., and H. W. BEAMS. 1960. Cytological observations on the fine structure of the guinea pig ovary with special reference to the oogonium, primary oocyte and associated follicle cells. *J. Ultrastruct. Res.* **3**:432.
3. ANDRÉ, J. 1962. La morphologie des mitochondries est une propriété fondamentale de la cellule en rapport avec son organisation. *J. Ultrastruct. Res.* **6**(Suppl. 3):1.
4. BATTIFORA, H., R. EISENSTEIN, G. H. LAING, and P. MCCREARY. 1966. The kidney in experimental magnesium deprivation. A morphologic and biochemical study. *Am. J. Pathol.* **48**:421.
5. BLINZINGER, K., N. B. REWCASTLE, and H. HAGER. 1965. Observations on prismatic-type mitochondria within astrocytes of the Syrian hamster brain. *J. Cell Biol.* **25**:293.
6. EBE, T., S. KOBAYASHI, and T. YAMAMOTO. 1965. Intramitochondrial inclusion bodies in the urinary epithelium of striped snake (*Elaphe quadrivirgata*). *J. Electronmicroscopy* (*Tokyo*). **14**:203.
7. EKHOLM, R., and Y. EDLUND. 1958. The mitochondria in human normal and cholestatic liver. *In* Proceedings of the Fourth International Conference for Electron Microscopy. W. Bargmann, D. Peters, and C. Wolpers, editors. Springer-Verlag, Berlin. **2**:273–275.
8. ELLIOTT, A. M., and I. J. BAK. 1964. The fate of mitochondria during aging in *Tetrahymena pyriformis*. *J. Cell Biol.* **20**:113.
9. FAWCETT, D. W., and S. ITO. 1958. Observations on the cytoplasmic membranes of testicular cells, examined by phase contrast and electron microscopy. *J. Biophys. Biochem. Cytol.* **4**:135.
10. FAWCETT, D. W. 1961. The membranes of the cytoplasm. *Lab. Invest.* **10**:1162.
11. FINEAN, J. B. 1959. Electron microscope and x-ray diffraction studies of a saturated synthetic phospholipide. *J. Biophys. Biochem. Cytol.* **6**:123.
12. FREI, J. V., and H. SHELDON. 1961. Corpus intra cristam: a dense body within mitochondria of cells in hyperplastic mouse epidermis. *J. Biophys. Biochem. Cytol.* **11**:724.
13. FUJITA, H., and M. MACHINO. 1964. Fine structure of intramitochondrial crystals in rat thyroid follicular cell. *J. Cell Biol.* **23**:383.
14. HUXLEY, H. E., and G. ZUBAY. 1961. Preferential staining of nucleic acid-containing structures for electron microscopy. *J. Biophys. Biochem. Cytol.* **11**:273.
15. ISERI, O. A., C. S. LIEBER, and L. S. GOTTLIEB. 1966. The ultrastructure of fatty liver induced by prolonged ethanol ingestion. *Am. J. Pathol.* **48**:535.
16. JEZEQUEL, A. M. 1959. Dégénérescence myélinique des mitochondries de foie humain dans un épithélioma du cholédoque et un ictère viral. Etude au microscope électronique. *J. Ultrastruct. Res.* **3**:210.
17. LAGUENS, R., and N. BIANCHI. 1963. Fine struc-

ture of the liver in human idiopathic diabetes mellitus. I. Parenchymal cell mitochondria. *Exptl. Mol. Pathol.* **2**:203.

18. LUFT, J. H. 1961. Improvements in epoxy resin embedding methods. *J. Biophys. Biochem. Cytol.* **9**:409.
19. LUFT, R., D. IKKOS, G. PALMIERI, L. ERNSTER, and B. AFZELIUS. 1962. A case of severe hypermetabolism of nonthyroid origin with a defect in the maintenance of mitochondrial respiratory control: a correlated clinical, biochemical and morphological study. *J. Clin. Invest.* **41**:1776.
20. MILLONIG, G. 1961. A modified procedure for lead staining of thin sections. *J. Biophys. Biochem. Cytol.* **11**:736.
21. MINICK, O. T., G. KENT, E. ORFEI, and F. I. VOLINI. 1965. Non-membrane enclosed intramitochondrial dense bodies. *Exptl. Mol. Pathol.* **4**:311.
22. MUGNAINI, E. 1964. Filamentous inclusions in the matrix of mitochondria from human livers. *J. Ultrastruct. Res.* **11**:525.
23. MUGNAINI, E., and F. WALBERG. 1964. Ultrastructure of neuroglia. *Ergeb. Anat. Entwicklungsgesch.* **37**:194.
24. MUGNAINI, E. 1964. Helical filaments in astrocytic mitochondria of the corpus striatum in the rat. *J. Cell Biol.* **23**:173.
25. NAPOLITANO, L., and D. W. FAWCETT. 1958. The fine structure of brown adipose tissue in the newborn mouse and rat. *J. Biophys. Biochem. Cytol.* **4**:685.
26. NASS, M. M. K., and S. NASS. 1962. Fibrous structures within the matrix of developing chick embryo mitochondria. *Exptl. Cell Res.* **26**:424.
27. NASS, M. M. K., and S. NASS. 1963. Intramitochondrial fibers with DNA characteristics. I. Fixation and electron staining reactions. *J. Cell Biol.* **19**:593.
28. NASS, S., and M. M. K. NASS. 1963. Intramitochondrial fibers with DNA characteristics. II. Enzymatic and other hydrolytic treatments. *J. Cell Biol.* **19**:613.
29. NILSSON, O. 1958. Ultrastructure of mouse uterine surface epithelium under different estrogenic influences. I. Spayed animals and oestrous animals. *J. Ultrastruct. Res.* **1**:375.
30. NOVIKOFF, A. B. 1961. Mitochondria (chondriosomes). *In* The Cell: Biochemistry, Physiology, Morphology. J. Brachet and A. E. Mirsky, editors. Academic Press Inc., New York. **2**:299–421.
31. PAPPAS, G. D., and P. W. BRANDT. 1959. Mitochondria. I. Fine structure of the complex patterns in the mitochondria of *Pelomyxa carolinensis* Wilson (*Chaos chaos* L.). *J. Biophys. Biochem. Cytol.* **6**:85
32. PAPPAS, G. D. 1959. Electron microscope studies on amoebae. *Ann. N. Y. Acad. Sci.* **78**:448.
33. PORTA, E. A., W. S. HARTROFT, and F. A. DE LA IGLESIA. 1965. Hepatic changes associated with chronic alcoholism in rats. *Lab. Invest.* **14**:1437.
34. REICHEL, J., S. B. GOLDBERG, M. ELLENBERG, and F. SCHAFFNER. 1960. Intrahepatic cholestasis following administration of chlorpropamide. Report of a case with electron microscopic observations. *Am. J. Med.* **28**:654.
35. REVEL, J. P., D. W. FAWCETT, and C. W. PHILPOTT. 1963. Observations on mitochondrial structure. Angular configurations of the cristae. *J. Cell Biol.* **16**:187.
36. SCHAFFNER, F., A. LOEBEL, H. A. WEINER, and T. BARKA. 1963. Hepatocellular cytoplasmic changes in acute alcoholic hepatitis. *J. Am. Med. Assoc.* **183**:343.
37. SCHUSTER, F. L. 1965. A deoxyribose nucleic acid component in mitochondria of *Didymium nigripes*, a slime mold. *Exptl. Cell Res.* **39**:329.
38. SORENSON, G. D., W. A. HEEFNER, and J. B. KIRKPATRICK. 1964. Experimental amyloidosis. II. Light and electron microscopic observations of liver. *Am. J. Pathol.* **44**:629.
39. SREBRO, Z. 1965. The ultrastructure of gliosomes in the brains of amphibia. *J. Cell Biol.* **26**:313.
40. STOECKENIUS, W. 1959. An electron microscope study of myelin figures. *J. Biophys. Biochem. Cytol.* **5**:491.
41. STOECKENIUS, W. 1961. Electron microscopy of DNA molecules "stained" with heavy metal salts. *J. Biophys. Biochem. Cytol.* **11**:297.
42. SVOBODA, D. J., and R. T. MANNING. 1964. Chronic alcoholism with fatty metamorphosis of the liver. Mitochondrial alterations in hepatic cells. *Am. J. Pathol.* **44**:645.
43. SVOBODA, D. J., and J. HIGGINSON. 1964. Ultrastructural changes produced by protein and related deficiencies in the rat liver. *Am. J. Pathol.* **45**:353.
44. THIERY, J. P., and J. CAROLI. 1962. Etude comparative en microscopie électronique de l'amylose hépatique primaire humaine et de l'amylose expérimentale de la souris. *Rev. Intern. Hepatol.* **12**:207.
45. WATSON, M. L. 1958. Staining of tissue sections for electron microscopy with heavy metals. *J. Biophys. Biochem. Cytol.* **4**:475.
46. WILLS, E. J. 1965. Crystalline structures in the mitochondria of normal human liver parenchymal cells. *J. Cell Biol.* **24**:511.
47. YAMAMOTO, I. 1966. Ultrastructural changes in mesenteric lymph nodes of mice infected with *salmonella enteritidis*. *J. Infect. Diseases.* **116**:8.